Hu Huang,[1] Jianbo He,[1,2] Da'Kuawn Johnson,[1] Yanhong Wei,[1] Ying Liu,[1,3] Shuang Wang,[1,4] Gerard A. Lutty,[1] Elia J. Duh,[1] and Richard D. Semba[1]

Deletion of Placental Growth Factor Prevents Diabetic Retinopathy and Is Associated With Akt Activation and HIF1α-VEGF Pathway Inhibition

Diabetes 2015;64:200–212 | DOI: 10.2337/db14-0016

COMPLICATIONS

A new diabetic mouse strain, the Akita.PlGF knockout ($^{-/-}$), was generated to study the role of placental growth factor (PlGF) in the pathogenesis of diabetic retinopathy (DR). PlGF deletion did not affect blood glucose but reduced the body weight of Akita.PlGF$^{-/-}$ mice. Diabetes-induced retinal cell death, capillary degeneration, pericyte loss, and blood-retinal barrier breakdown were prevented in these mice. Protein expression of PlGF was upregulated by diabetes, particularly in vascular cells. Diabetes-induced degradation of ZO-1 and VE-cadherin was reversed due to PlGF deficiency; their expression was correlated with that of sonic hedgehog and angiopoietin-1. PlGF deletion in Akita mice resulted in an increased Akt phosphorylation. Diabetes-activated hypoxia-inducible factor (HIF)1α–vascular endothelial growth factor (VEGF) pathway, including expression of HIF1α, VEGF, VEGFR1–3, and the extent of phospho (p)-VEGFR1, p-VEGFR2, and p–endothelial nitric oxide synthase, was inhibited in the retinas of diabetic PlGF$^{-/-}$ mice. However, expression of intercellular adhesion molecule-1, vascular cell adhesion molecule-1, CD11b, and CD18 was not inhibited by PlGF deletion, nor was retinal leukostasis. These results suggest that PlGF is critical for the development of DR, and its genetic deletion protects the retina from diabetic damage. Protective mechanisms are associated with Akt activation and HIF1α-VEGF pathway inhibition, but independent of retinal leukostasis in the retinas of diabetic PlGF$^{-/-}$ mice.

Diabetic retinopathy (DR) is a leading cause of visual impairment and blindness. DR is characterized by increased vascular permeability; breakdown of the blood-retinal barrier (BRB); apoptotic cell death of retinal neurons, endothelial cells (ECs), and pericytes; and the appearance of microaneurysms and acellular capillaries. Several biological pathways have been implicated in the pathogenesis of DR, including vascular endothelial growth factor (VEGF) (1), tumor necrosis factor-α (2), the kallikrein-kinin system (3), and altered *O*-GlcNAc signaling (4). The exact mechanisms and the relationship of pathogenic changes to biochemical pathways in DR need further elucidation.

Placental growth factor (PlGF), a member of the VEGF family, was first described from a human placental cDNA library in 1991 (5). PlGF is expressed by a wide variety of cell types, including ECs and retinal pigment epithelial cells (RPEs) in response to hypoxia (6,7). PlGF is a homolog of VEGF and binds to fms-like tyrosine kinase-1 (FLT1; also known as VEGFR-1) and soluble FLT1,

[1]Wilmer Eye Institute, Johns Hopkins University School of Medicine, Baltimore, MD
[2]Guangxi Tumor Hospital and Institute, Nanning, Guangxi, China
[3]Aier Eye Hospital, Changsha, Hunan, China
[4]China Japan Union Hospital, Changchun, Jilin, China
Corresponding author: Hu Huang, hhuang27@jhmi.edu.

Received 5 January 2014 and accepted 21 July 2014.

This article contains Supplementary Data online at http://diabetes.diabetesjournals.org/lookup/suppl/doi:10.2337/db14-0016/-/DC1.

a circulating form of FLT1 that lacks the transmembrane and intracellular domains. Activation of FLT1 by PlGF augments the effects of VEGF signaling with VEGFR-2, suggesting synergistic effects of PlGF and VEGF (8,9). PlGF can also form heterodimers with VEGF (8). PlGF exerts a strong effect upon blood vessel growth and maturation and has direct proangiogenic effects on ECs (6).

Recent studies suggest that PlGF plays a role in the pathogenesis of DR (10). Diabetic human retinas have higher expression of PlGF mRNA compared with nondiabetic retinas (11). In proliferative DR, immunoreactivity for PlGF was localized to endothelial and perivascular regions of neovascular membranes (12). PlGF was produced in a cultured human RPE line in response to hypoxia (13). Other studies have shown higher concentrations of PlGF in aqueous and vitreous humor of eyes with DR compared with controls (14–16).

Mice with inactivation of the gene expressing PlGF (*plgf*$^{-/-}$ or *pgf*$^{-/-}$) show little effect of PlGF absence on vascular development, but in response to hypoxia, PlGF$^{-/-}$ mice have reduced angiogenesis in the retina from oxygen-induced retinopathy (6). The findings from clinical studies, in vitro studies, and PlGF$^{-/-}$ mice demonstrate the PlGF may have a role in the pathogenesis of DR. To gain further insights, we compared molecular and histological changes in wild-type (WT) mice, Akita diabetic mice, and PlGF$^{-/-}$ mice and generated a novel Akita.PlGF$^{-/-}$ mouse strain. We hypothesized that DR would be less severe in Akita diabetic mice that were deficient in PlGF.

RESEARCH DESIGN AND METHODS

Diabetic Mice

Animal use was in accordance with the approved protocols by the Institutional Animal Care and Use Committee of The Johns Hopkins University. Akita mice were crossed with PlGF$^{-/-}$ mice (17) in a C57BL/6J background for two generations to give birth to the progeny with the genotype of Akita.PlGF$^{-/-}$. Additional mating of Akita.PlGF$^{-/-}$ and PlGF$^{-/-}$ was performed to fix the PlGF mutation to homozygosity while maintaining the Akita mutation in the heterozygous state. The genotyping of PlGF gene was performed as described in the literature (6). The genotyping for Pde6b^{rd1} and Crb1^{rd8} genes was performed as described in the literature (18,19).

Western Blots and Quantification

Western blot (WB) was performed as described previously (20). The anti-PlGF, anti–hypoxia-inducible factor (HIF)-1α, anti-VEGFR1, anti-VEGFR2, anti–intercellular adhesion molecule (ICAM)-1, anti–vascular cell adhesion molecule (VCAM)-1, anti-ZO-1, and anti-VE-cadherin antibodies are described in more detail elsewhere (21,22). Dilutions of 1:200 and 1:1,000 were used for anti-VEGF antibody (Santa Cruz, Dallas, TX) and anti-VEGFR3 antibody (eBioscience, San Diego, CA), respectively. The anti-Akt and anti-phospho (p)-Akt antibodies were bought from Cell Signaling (Indiana, IN) and used as 1:1,000 dilutions.

The optical density (OD) of protein bands in WB images was determined by ImageJ (National Institutes of Health). After normalization by dividing the OD of protein of interest with the housekeeping gene β-actin of the same sample, the percentage of the normalized OD was calculated for each protein of interest based on this equation: percentage of OD (4) = 100*OD (4) / [OD (1) + OD (2) + OD (3) + OD (4)] (each represents one retinal protein sample in the same WB membrane). The average percentage of normalized OD was designated as the relative protein expression (n = 6).

Apoptotic Cell Death Assays

The methods of TUNEL assay were described previously (2). Apoptotic DNA cleavage was analyzed with the cell death ELISA kit (Roche, Indianapolis, IN), which was performed according to the manufacturer's instructions with some modifications. In brief, retina was incubated with lysis buffer (0.1 mol/L citric acid buffer containing 0.5% Tween 20) for 30 min. Retinal lysates were centrifuged to sediment the cell debris and nuclei (>1,500 rpm, for 10 min). The 20 μL supernatants were subjected to apoptotic DNA cleavage ELISA assay. The OD (absorbance at 405 nm with a reference at 490 nm) was normalized with retinal mass. The average OD/retinal mass indicated the level of cytoplasmic nucleosome containing fragmented DNA (n = 8).

Transcardial Perfusion, Confocal Microscopy, and Retinal Leukostasis

The transcardial perfusion of fluorescein isothiocyanate (FITC)-dextran and confocal microscopy were performed as described previously (21). The z-series of optical sections from confocal images were made of the superficial, intermediate, and deep retinal vessel bed to examine the localization of FITC-dextran (70 kDa, TdB Consultancy, Sweden). Retinal leukostasis was performed as previously described (2).

Quantitative BRB Assay

The quantitative BRB assay was performed as previously described (2,21). The count per minute (CPM) was normalized with tissue weight (CPM/mg retina, lung, or kidney) or with serum volume (CPM/μL/h). The ratio of retina to lung, kidney, or serum was designated as retinal vascular leakage ratio.

Immunofluorescence Staining and Quantification

Immunofluorescence (IF) staining was performed as described previously (22). The primary antibodies used for this study included anti-CD31/PECAM-1 (BD Pharmingen, San Jose, CA); anti-VEGFR1 (ImClone, Somerville, NJ); and anti-p-VEGFR1 (Y1213; R&D Systems), anti-NG2, anti-GFAP, anti-p-Akt (Ser473), anti-p-VEGFR2 (Tyr1175), and anti-p-endothelial nitric oxide synthase (eNOS; Ser1177; Cell Signaling). For double labeling, two primary antibodies from the distinct host species

were mixed for the same tissue section and two appropriate secondary antibodies conjugated with different chromophores (e.g., rhodamine or fluorescein) were used for detection and visualization. For the quantitative comparison of IF images, the specimens and images were prepared as described previously (23). The immunoreactive intensity and area were quantified by ImageJ and Image Pro, respectively.

Real-Time PCR

The procedures of real-time PCR were described previously (20,24). For quantifying the relative expression of genes of interest (GOI), the threshold cycles (*C*t) were normalized by subtracting the Ct of housekeeping gene actin of the same sample (ΔCt = GOI *C*t-actin *C*t). The value of $2^{-\Delta Ct}$ was calculated for each sample and average for each mouse strain. The percentage of the average $2^{-\Delta Ct}$ from each mouse strain to the sum $2^{-\Delta Ct}$ from the four mouse strains was designated as the relative expression of GOI (n = 6).

Trypsin Digestion and Quantification

Isolation of retinal vasculature and quantification of acellular capillary were performed as previously described (25,26). The enucleated eyes were fixed with 2% paraformaldehyde for 24 h. After removing the cornea, the eye cups were fixed with 2% paraformaldehyde for 24 h and dissected to isolate the retina. The retinas were rinsed in tap water overnight and then were incubated with 40 unit/mL elastase (Calbiochem, MA) in 100 mmol/L sodium phosphate buffer with 150 mmol/L sodium chloride and 5.0 mmol/L EDTA pH 6.5 at 37°C for 2 h. Retinas were transferred to a 100 mmol/L Tris-HCl (8.5) solution at room temperature for 3 h. Nonvascular tissues were removed by gentle brushing, and the isolated vasculature was mounted on the slide. After drying overnight, the retinal blood vessels were subjected to the periodic acid–Schiff and hematoxylin stain. The retinal blood vessels of 20–25 random fields (200× magnification) were analyzed in a masked fashion for the quantification of acellular capillaries, which were identified as capillary-sized vessel tubes without nuclei along their length. The numbers were normalized by the counting area (degenerated vessels/mm^2). The number of ECs and pericytes were determined by counting their respective nuclei, the differences of which were distinguished by their morphology and position in the blood vessels, as described previously (27). The six midzone fields of retinal digest (400× magnification) were analyzed for each retina in a masked fashion. The average number of ECs per mm^2 vascular bed was calculated and expressed as the density of EC. The average ratio of EC to pericyte was used to demonstrate the pericyte coverage or death.

Statistical Analysis

The nonparametric Mann-Whitney *U* test was performed to determine the significance level between two samples: diabetic retina versus nondiabetic retina and Akita versus Akita.PlGF$^{-/-}$. $P < 0.05$ was designated as being statistically significant.

RESULTS

Blood Glucose Is Not Affected, but Body Weight Is Reduced in Akita.PlGF$^{-/-}$ Mice

We generated a genetic model of diabetes by crossing the PlGF$^{-/-}$ mouse and the Akita diabetic mouse. PCR genotyping analysis confirmed the deletion of the PlGF gene in Akita.PlGF$^{-/-}$ mice (Fig. 1*A*). We further performed genotyping for Pde6b^{rd1} and Crb1^{rd8} genes, since the two are common retinal degeneration gene mutations that are found in the C57BL/6 mouse strains (18). The results showed that neither was present in the four mouse strains used in this study. Further histopathological analysis indicated there was no obvious retinal degeneration, as indicated by the 10–12 nuclear layers in photoreceptors, and other retinal abnormalities (Supplementary Fig. 1). The level of blood glucose was equal between the offspring of WT/Akita (PlGF$^{+/+}$/Akita.PlGF$^{-/-}$) and PlGF$^{-/-}$/Akita.PlGF$^{-/-}$ breeding mice (Fig. 1*B* and *C*). The Akita.PlGF$^{-/-}$ mice were significantly lighter in body weight than the same-aged Akita mice (Fig. 1*D* and Supplementary Table 1). Despite the loss of body weight, the double mutant Akita.PlGF$^{-/-}$ mice were viable, fertile, and healthy. The blood assays and histopathological assessments also suggested less severe pathology in the liver and kidney of Akita.PlGF$^{-/-}$ mice than Akita mice (data not shown).

Cell Death Is Decreased in the Retinas of Akita.PlGF$^{-/-}$ Mice

By comparing the two diabetic mouse strains (Akita and Akita.PlGF$^{-/-}$) with their respective nondiabetic mouse strains of the same genetic background (C57BL6 [WT] and PlGF$^{-/-}$ mice), we found that PlGF deficiency prevented diabetes-caused retinal cell death in the Akita.PlGF$^{-/-}$ mouse retina. The number of diabetes-induced TUNEL(+) cells was significantly reduced in Akita.PlGF$^{-/-}$ mice compared with Akita mice of the same age (Fig. 2*A*–*E*). The number of activated caspase-3(+) cells was also significantly reduced due to PlGF deficiency in the diabetic retina (data not shown). Furthermore, apoptotic cell death was examined by cell death ELISA analysis, in which cytoplasmic nucleosomes were measured. The results showed that DNA fragmented nucleosomes were increased in Akita diabetic mice compared with nondiabetic mice, but not in Akita.PlGF$^{-/-}$ mice (Fig. 2*F*).

Capillary Degeneration and Pericyte Death Are Abrogated in the Retinas of Akita.PlGF$^{-/-}$ Mice

Retinal digests were performed as described in RESEARCH DESIGN AND METHODS. Intact retinal vasculatures were used for quantitative analyses of acellular capillary, EC density, and pericyte death. Firstly, acellular capillaries or capillary degeneration were significantly increased in Akita mice compared with WT controls. Genetic ablation of the PlGF gene abrogated the diabetes-induced capillary degeneration: the mean number of acellular capillary/mm^2

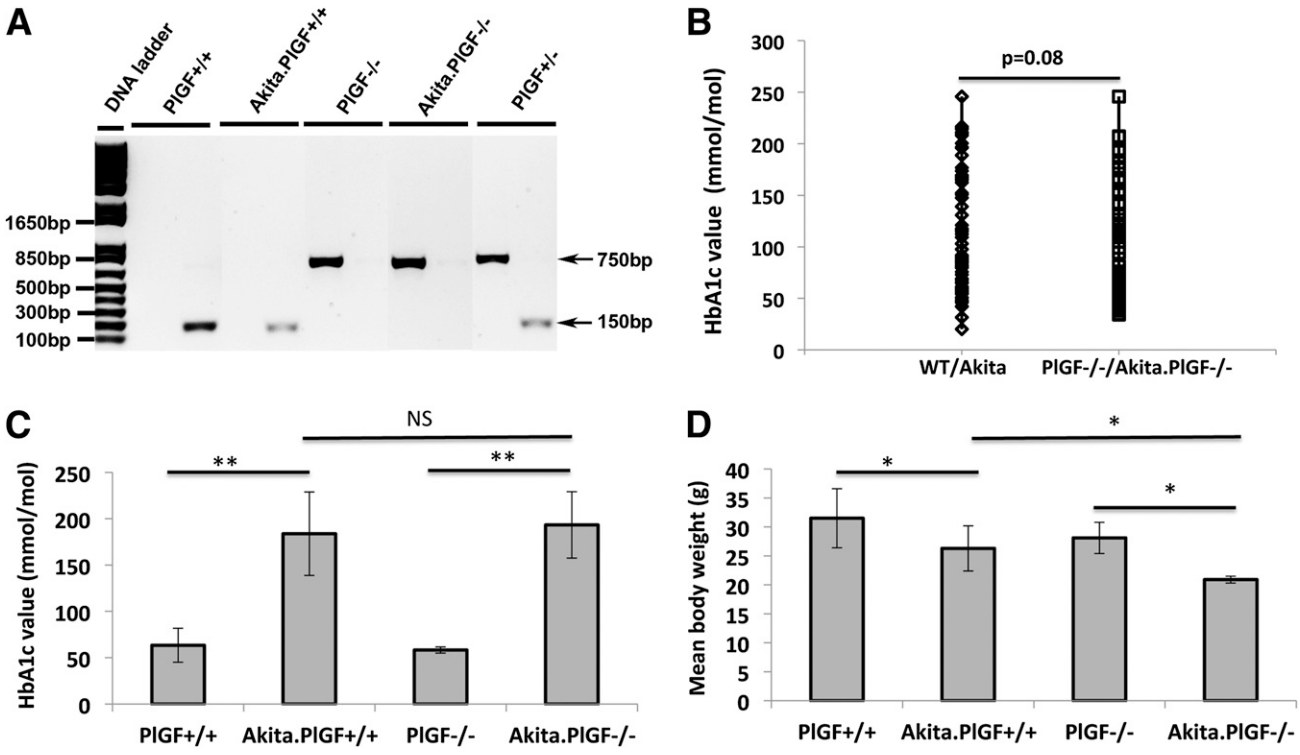

Figure 1—The blood glucose and body weight of Akita.PlGF$^{-/-}$ mice. *A*: The PCR genotyping results for PlGF$^{+/+}$ (WT), Akita.PlGF$^{+/+}$ (Akita), PlGF$^{-/-}$, and Akita.PlGF$^{-/-}$. The PCR products of PlGF heterozygous (+/−) mice indicated the amplicons of 750 bp ($^{-/-}$) and 150 bp ($^{+/+}$). *B*: The blood glucose level of the offspring of WT/Akita breeding mice or PlGF$^{-/-}$/Akita.PlGF$^{-/-}$ breeding mice. The blood glucose of 95 ~1-month-old male mice (diabetes just started) from WT/Akita breeding mice and 115 same-aged male mice from PlGF$^{-/-}$/Akita.PlGF$^{-/-}$ breeding mice was measured (mg/dL), converted to the HbA_{1c} values (mmol/mol), and then scatter plotted. *C*: The average body weight and blood glucose (see Supplementary Table 1 for the values of HbA_{1c} % and mmol/mol) of 6-month-old diabetic male mice (5-month diabetes duration) and their nondiabetic littermate male mice (n = 10). Blood glucose of 250 mg/dL was used as the cutoff for diabetic and nondiabetic mice. *P < 0.05; **P < 0.0001.

retinal vasculature was significantly increased in Akita mice compared with WT and Akita.PlGF$^{-/-}$ mice. Secondly, there was not a significant change in the density of vascular ECs between the mouse strains (Supplementary Fig. 2 and Supplementary Table 2). Lastly, pericyte death was significantly increased in Akita mice compared with WT mice, but PlGF deletion abrogated diabetes-induced pericyte loss (Fig. 3). Consistently, double immunostaining of NG2 and CD31 showed the pericyte coverage was decreased by diabetes (5-month diabetes duration), but PlGF deletion abrogated the pericyte loss: the average ratio of NG2(+) to CD31(+) vessel areas was significantly reduced in Akita diabetic retina compared with the nondiabetic control retina, but that of Akita.PlGF$^{-/-}$ retina was not (Supplementary Fig. 3).

Although it is possible that PlGF, like its homolog VEGF, is produced by a variety of retinal cell types, its cellular targets appear to be vascular ECs and pericytes in diabetic retina. We investigated this question with the vascular EC markers CD31 and the pericyte marker NG2. IF staining also showed an increased expression of PlGF protein and its receptor VEGFR1 by diabetes: PlGF or VEGFR1 immunoreactivity was not present or, if present, was barely detectable in nondiabetic mouse retina but was dramatically increased in the retinas of Akita diabetic mice (3 months old with an ~2-month diabetes duration). Double labeling of IF staining showed that the diabetes-induced increased PlGF protein colocalizes well with its receptor VEGFR1, the EC marker CD31, and the pericyte marker NG2 but does not colocalize with the astrocyte/glial marker GFAP (Supplementary Fig. 4). These results suggest vascular EC and pericytes are likely the cellular targets of PlGF, where it mediates DR by transmitting signaling via VEGFR1. We recently observed that diabetes-induced inflammation and vascular leakage were significantly inhibited due to VEGFR1 blockade (J.H., D. Kim, and H.H., unpublished data).

Vascular Leakage Is Prevented in the Retinas of Akita.PlGF$^{-/-}$ Mice

Vascular leakage was determined by a quantitative BRB method, in which ^{3}H-mannitol (molecular weight 182 Da) acted as a tracer. The results showed diabetes caused a significant vascular leakage in Akita mice compared with the nondiabetic control mice, which is consistent with our previous results (2). However, deletion of PlGF in Akita mice prevented diabetes-related vascular leakage (Fig. 4). Vascular leakage was further examined by the

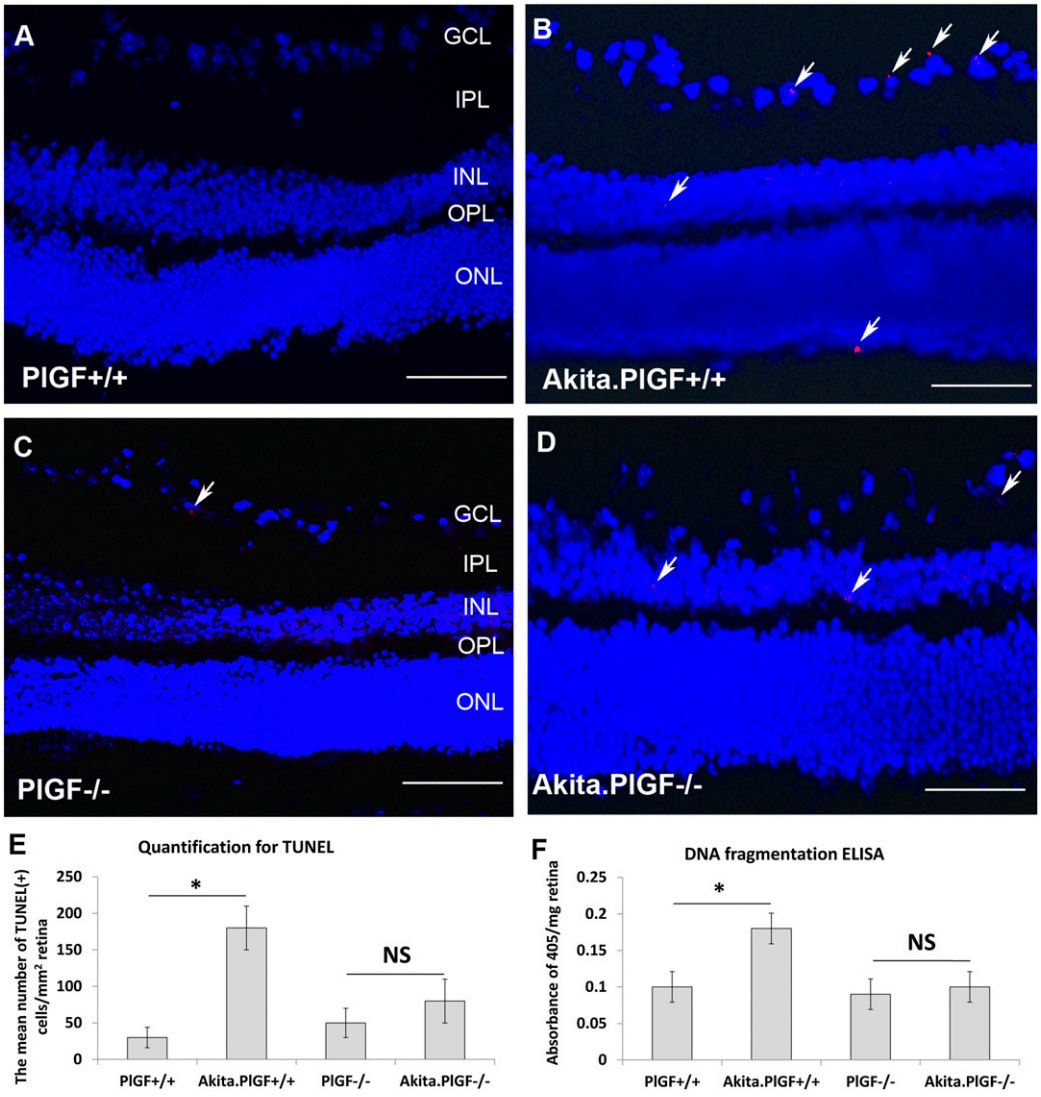

Figure 2— Decreased cell death in the retinas of Akita.PlGF$^{-/-}$ mice. Cryopreserved eye sections were made from the 6-month-old diabetic male mice (~5-month diabetes duration) and nondiabetic littermate male mice. Cell death was detected by TUNEL staining. *A–D*: The example results of TUNEL staining for WT (*A*), Akita (*B*), PlGF$^{-/-}$ (*C*), and Akita.PlGF$^{-/-}$ (*D*). *E*: Quantification of the TUNEL(+) cells. Results were shown as mean ± SD of TUNEL(+) cells per mouse strain (n = 6). *F*: The cell death ELISA. The results were averaged from eight measurements and expressed as mean ± SD (n = 8). *$P < 0.05$; NS, not significant. GCL, ganglion cell layer; INL, inner nuclear layer; IPL, inner plexiform layer; ONL, outer nuclear layer.

extravascularization of FITC-dextran (70 kDa) in the superficial (ganglion cell layer), intermediate (inner plexiform layer), and deep (outer plexiform layer [OPL]) retinal vasculatures. The z-series of images by scanning confocal microscopy showed that the leakage of the perfused dextran could be observed in some areas of all three layers of Akita mouse vasculature but not in those of nondiabetic mice or Akita.PlGF$^{-/-}$ mice (Supplementary Fig. 5).

Expression of ZO-1 and VE-Cadherin Is Upregulated in the Retinas of Akita.PlGF$^{-/-}$ Mice

We examined the expression of the tight junction protein ZO-1 and the adhesion protein VE-cadherin, both of which play critical roles in maintaining the integrity of BRB complex. The WB results showed that expression of the two proteins was significantly decreased in the Akita diabetic mice compared with the nondiabetic control mice, suggesting impaired BRB function. Protein expression was significantly increased in the Akita.PlGF$^{-/-}$ diabetic mouse retina compared with the nondiabetic PlGF$^{-/-}$ control mice, suggesting an enhanced BRB function (Fig. 5*A–D*). Furthermore, double labeling showed that ZO-1 colocalized with the vascular marker CD31/PECAM-1, similar to the nondiabetic PlGF$^{-/-}$ mice. However, the signal intensity and area of ZO-1 immunoreactivity were evidently reduced in Akita mice compared with those of CD31 (Supplementary Fig. 6). The mRNA expression of the two factors was consistent with their proteins: decreased in Akita mice, but increased in Akita.PlGF$^{-/-}$ mice (Fig. 5*E* and *F*). These results suggested PlGF

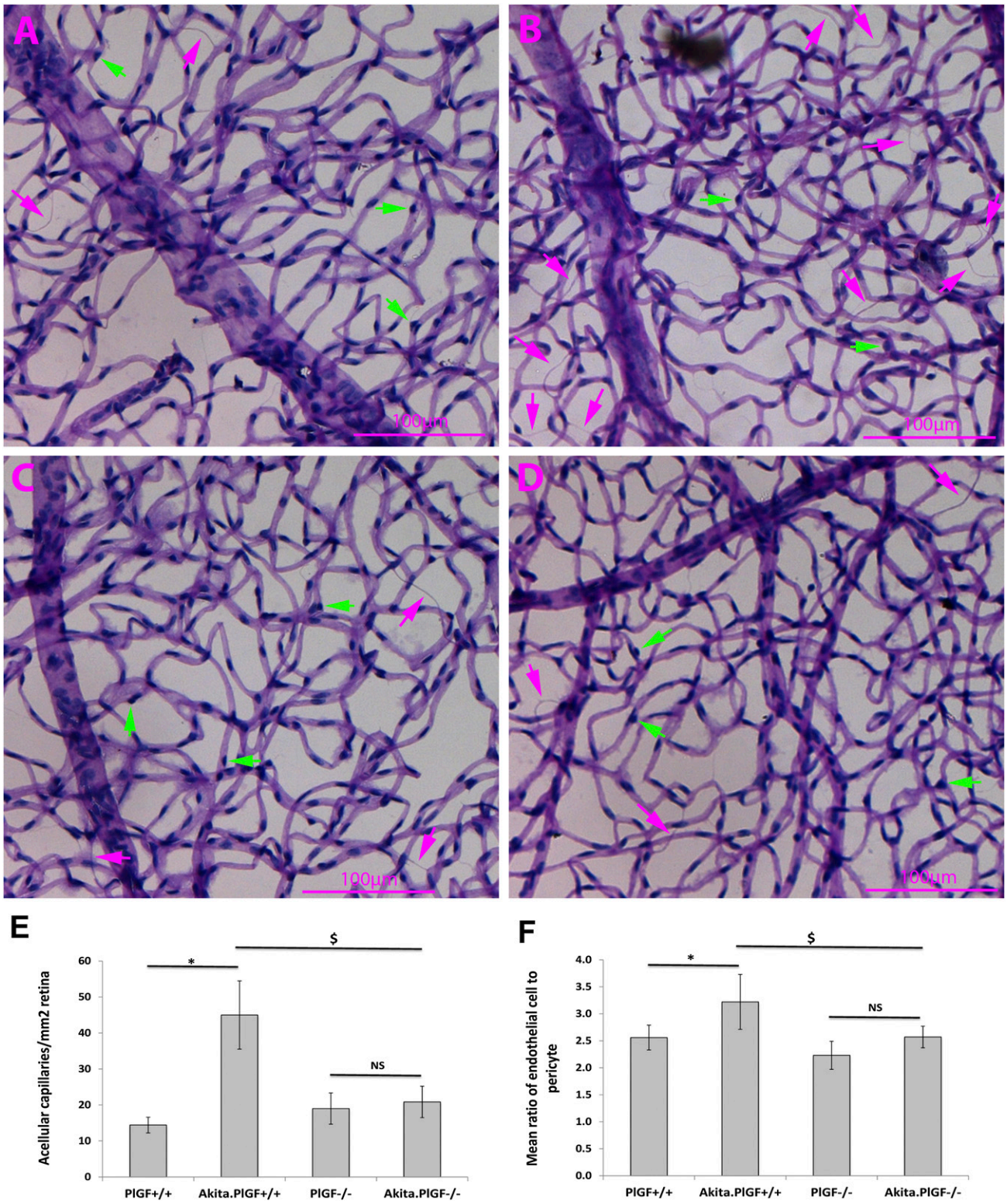

Figure 3—Decreased capillary degeneration and pericyte loss in the retinas of Akita.PlGF$^{-/-}$ mice. Six-month-old diabetic male mice (~5-month diabetes duration) and nondiabetic littermate male mice were used for elastase digestion. *A–D*: Representative examples of isolated retinal vasculature for PlGF$^{-/-}$ (*A*), Akita.PlGF$^{-/-}$ (*B*), WT (*C*), and Akita (*D*) mice strains. Purple arrows indicate acellular capillaries. Green arrows indicate pericytes. *E*: Quantification of acellular capillaries. Results were expressed as mean ± SD number of acellular capillaries/mm^2. *F*: Pericyte quantification. The results were expressed as the ratio of ECs to pericyte (n = 6). *P < 0.05 vs. nondiabetic WT control; \$$P$ < 0.05 vs. Akita diabetic mice; NS, not significant.

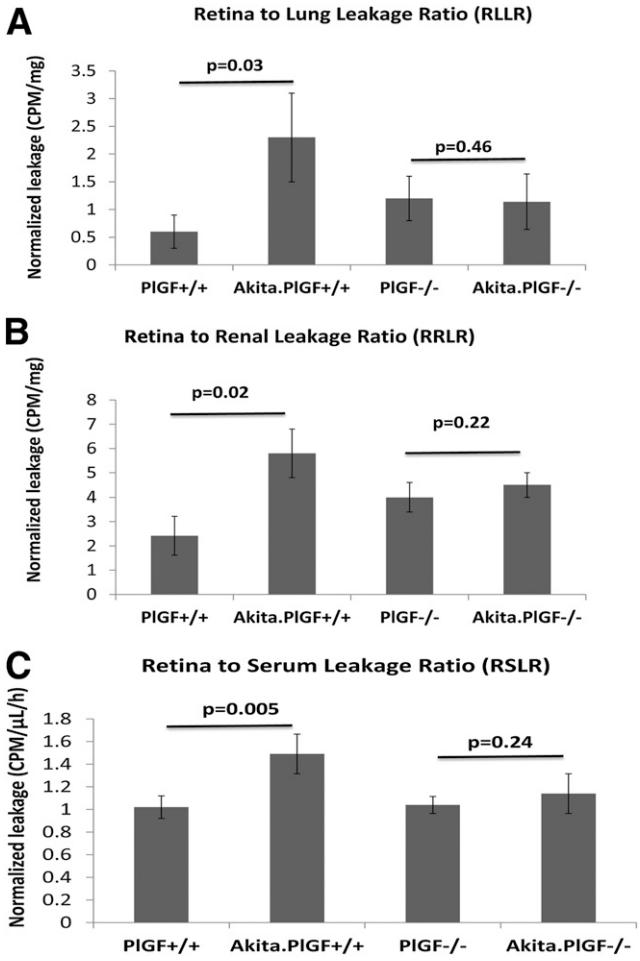

Figure 4— Decreased vascular leakage in the retinas of Akita.PlGF$^{-/-}$ mice. Six-month-old diabetic mice (~5-month diabetes duration) and age-matched nondiabetic littermate control mice were used for the quantitative BRB assay, in which ^{3}H-mannitol acts as a tracer. CPMs were normalized by the mass of tissues: retina, lung, and kidney (CPM/mg) or serum value (CPM/h/μL). Retina-to-lung leakage ratio (*A*), retina-to-renal leakage ratio (*B*), and retina-to-serum leakage ratio (*C*) were used to demonstrate the degree of vascular leakage.

deletion in Akita mice protects against diabetes-caused degradation of ZO-1 and VE-cadherin proteins and also upregulates both genes.

To give insight into the mechanisms regulating the increased expression of ZO-1 and VE-cadherin in these diabetic mouse retina, we examined mRNA expression of sonic hedgehog (SHH), angiopoietin (Ang)-1, activator protein-1, Sry-related HMG-box (Sox7), T-cell acute lymphocytic leukemia-1 (TAL1 or SCL), transcription factor 3 (TCL3 or E47), and LM02, all of which were known to regulate the expression of ZO-1 and/or VE-cadherin (28–30). We found that the expression of Ang-1 and SHH was concomitantly related with that of ZO-1 and VE-cadherin: decreased in Akita diabetic mouse retina, but increased in Akita.PlGF$^{-/-}$ compared with their respective nondiabetic control mice (Fig. 5*G* and *H*). The corelated expression patterns suggested that Ang-1 and SHH are likely involved in the regulation of ZO-1 and VE-cadherin expression in the diabetic conditions.

Akt Phosphorylation Is Increased in the Retinas of Akita.PlGF$^{-/-}$ Mice

Akt is a key survival factor that protects retinal cells from various impairments, including diabetes (31). We examined the extent and cellular localization of p-Akt, which is the activated form of Akt protein, by WB and IF staining. The WB results showed that Akt phosphorylation expressed in the WT mouse retina was abolished by diabetes (5-month diabetes duration) but was significantly increased in the retinas of Akita.PlGF$^{-/-}$ mice compared with its nondiabetic PlGF$^{-/-}$ control mouse retina (Fig. 6*A*). The p-Akt was not detected by IF staining in the retinas of the two nondiabetic mice or the Akita diabetic mice but was significantly increased in the retinas of Akita.PlGF$^{-/-}$ mice. p-Akt immunoreactivity was largely localized to the photoreceptor inner segment layer, outer nuclear layer and OPL in the PlGF$^{-/-}$ diabetic mouse retina (Fig. 6*B–E*). Interestingly, p-Akt immuoreactivity appeared to be present in the processes of Müller glial cells (Fig. 6*E* and *F*). The induction of Akt phosphorylation in these cell types suggests both autocrine and paracrine protective mechanisms may exist in the retinas of Akita.PlGF$^{-/-}$ mice.

HIF1α-VEGF Signaling Pathway Is Inhibited in the Retinas of Akita.PlGF$^{-/-}$ Mice

To investigate whether the HIF1α-VEGF signaling pathway is inhibited in Akita.PlGF$^{-/-}$ mice, we examined the expression of HIF1α, several VEGF family proteins (PlGF, VEGF-A, VEGF-B), and the three tyrosine kinase receptors (VEGFR1–3) in the Akita and Akita.PlGF$^{-/-}$ diabetic mice strains and their nondiabetic mouse controls. The WB results (Fig. 7*A* and *B*) showed that *1*) PlGF protein expression was negative in PlGF$^{-/-}$ and Akita.PlGF$^{-/-}$, further confirming the deletion of the PlGF gene in the PlGF$^{-/-}$ and Akita.PlGF$^{-/-}$ mouse strains; *2*) protein expression of HIF1α, PlGF, VEGF-A, and VEGFR1–3 was significantly upregulated in Akita mouse retina compared with the nondiabetic WT mouse retina, implicating the HIF1α-VEGF pathway in the pathogenesis of DR; *3*) protein expression of HIF1α, VEGF, and VEGFR1–3 was significantly downregulated in Akita.PlGF$^{-/-}$ mice compared with nondiabetic PlGF$^{-/-}$ mice, suggesting the inhibition of HIF1 α-VEGF pathway is likely one of the protective mechanisms; and *4*) VEGF-B protein expression was of the same level for all four mice stains, suggesting VEGF-B may not be involved in this type 1 diabetic model, although there is evidence supporting that VEGF-B is important in the type 2 diabetic model with obesity (32,33).

In addition, we examined the extent and cellular localization of the three important elements in the VEGF signaling pathway: p-VEGFR1, p-VEGFR2, and p-eNOS. Immunoreactivity of p-VEGFR1 and p-VEGFR2 prominently localized in the OPL; the signal intensity was increased in the retinas of Akita diabetic mice compared with the other three mouse strains. Double labeling

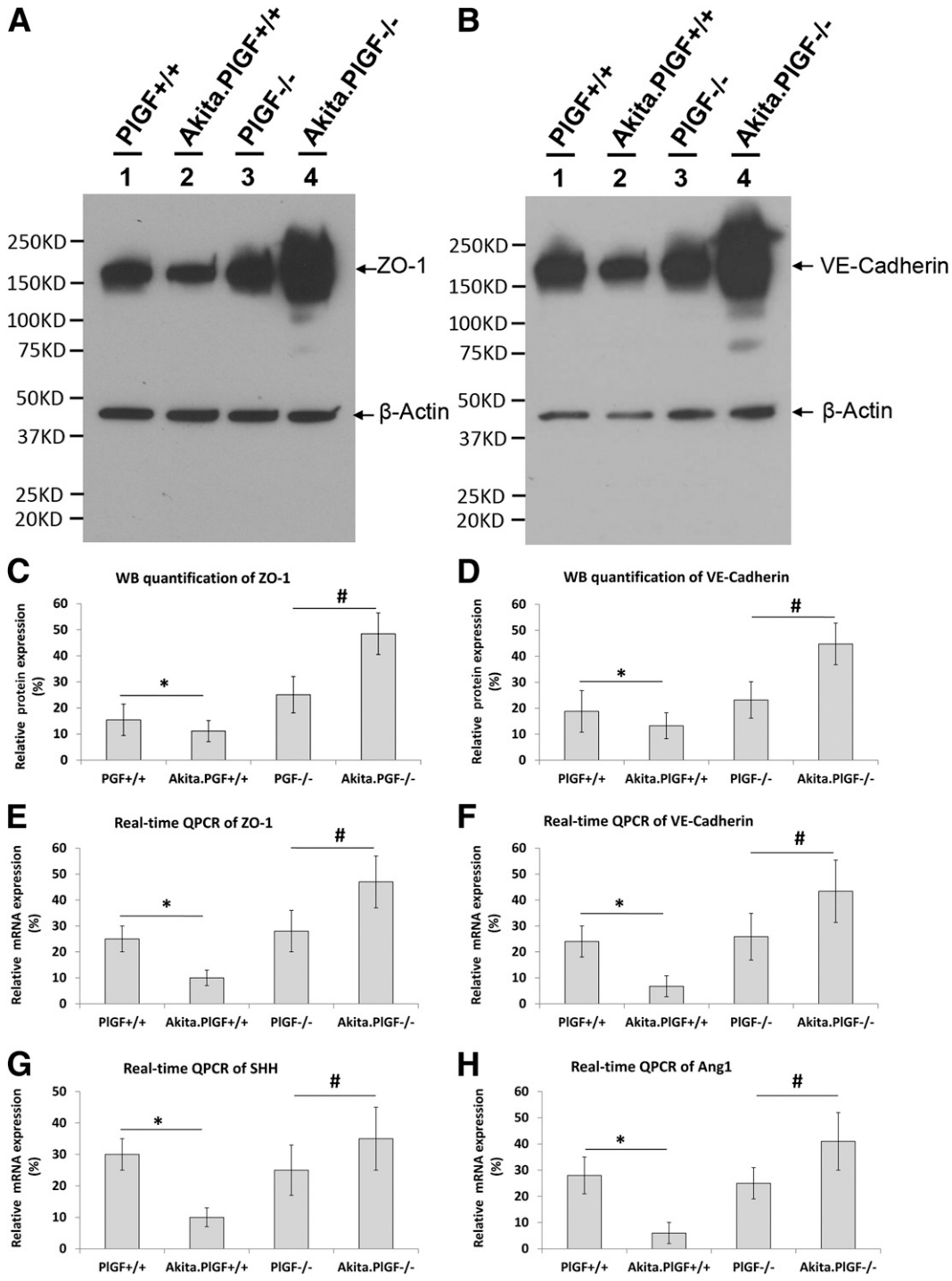

Figure 5—Increased expression of ZO-1, VE-cadherin, SHH, and Ang-1 in the retinas of Akita.PlGF$^{-/-}$ mice. Protein lysates and total RNA were prepared from the retinas of the 6-month-old mice diabetic mice (~5-month diabetes duration) and the littermate control mice. *A* and *B*: WB of ZO-1 (*A*) and VE-cadherin (*B*). Shown is the anti-β-actin antibody, which was mixed with anti-ZO-1 antibody or anti-VE-cadherin antibody and used to probe on the same protein membrane, serving as the internal control of protein loading and quantification. *C* and *D*: WB quantification of ZO-1 (*C*) and VE-cadherin (*D*). *E–H*: Relative mRNA expression of ZO-1 (*E*), VE-cadherin (*F*), SHH (*G*), and Ang-1 (*H*). The results were averaged from six results and expressed as the relative protein expression ± SD (n = 6). *P < 0.05 (Akita diabetic mice vs. WT nondiabetic mice); #P < 0.05 (Akita.PlGF$^{-/-}$ vs. PlGF$^{-/-}$). QPCR, quantitative PCR.

showed that p-VEGFR1-immunopositive(+) cells are either CD31(+) or CD31(−). The p-VEGFR1(+)/CD31(−) cells were present in all the four mouse strains, suggesting the constitutive expression, but the p-VEGFR1(+)/CD31(+) cells were only present in Akita diabetic mice, indicating the induced expression by diabetes (Fig. 7*C–F*). The expression pattern and cellular localization of p-VEGFR2 were similar to that of p-VEGFR1 (Fig. 7*G–J*). p-eNOS

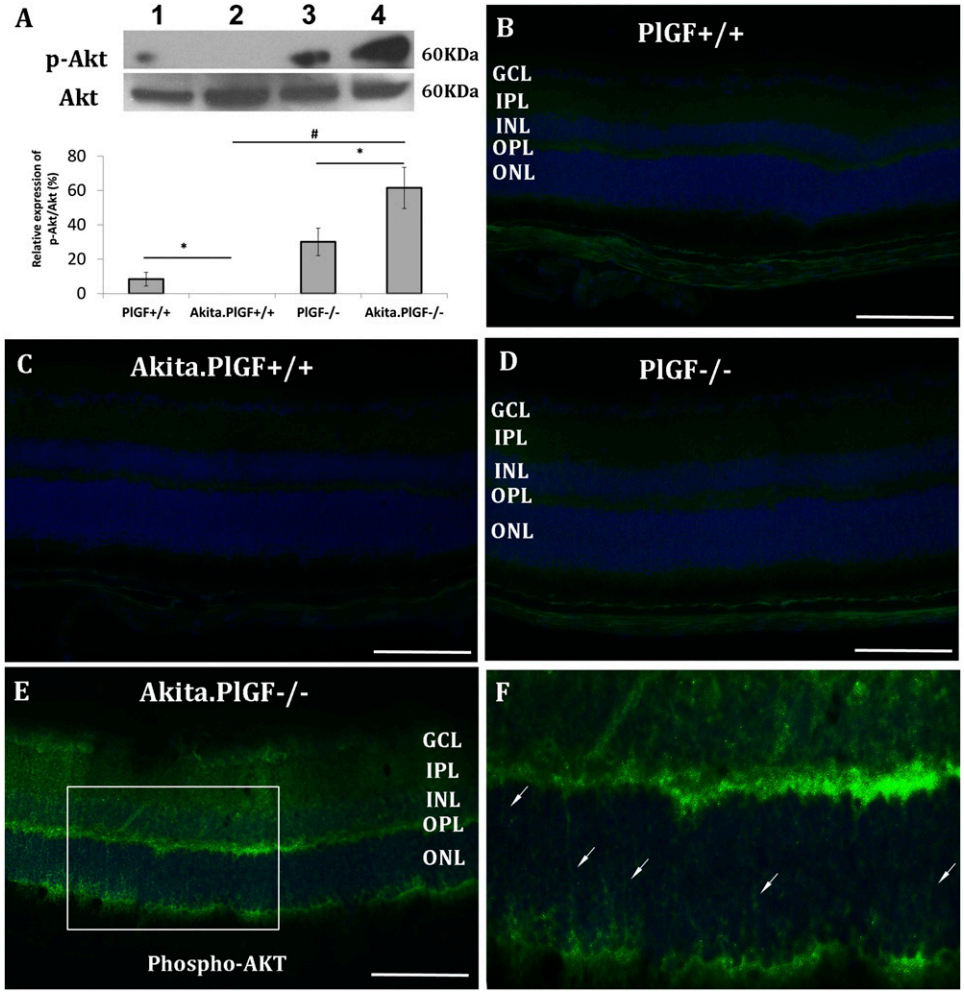

Figure 6—Increased Akt phosphorylation in the retinas of Akita.PlGF$^{-/-}$ mice. Six-month-old diabetic mice (~5-month diabetes duration) were compared with nondiabetic littermate control mice. *A*: The upper panel is the WB result of p-Akt and Akt protein; the lower panel is WB quantification, which is expressed as the percentage of p-Akt to Akt protein. Quantification of WB represents the average from six mice per mouse strain ($n = 6$). In the blot, lane 1 is nondiabetic WT (PlGF$^{+/+}$); lane 2 is Akita.PlGF$^{+/+}$; lane 3 is nondiabetic PlGF$^{-/-}$; and lane 4 is Akita.PlGF$^{-/-}$. *$P < 0.05$; #$P < 0.01$. IF staining of p-AKT on PlGF$^{+/+}$ (*B*), Akita (*C*), PlGF$^{-/-}$ (*D*), and Akita.PlGF$^{-/-}$ (*E*) is presented. Panel *F* is a high magnification of the boxed area in panel *E*. Arrows indicate the processes of Müller glial cells. Scale bar, 100 μm. GCL, ganglion cell layer; INL, inner nuclear layer; IPL, inner plexiform layer; ONL, outer nuclear layer.

was detected only in the Akita mice, not in the others; its immunoreactivity colocalized with CD31(+) cells or CD31(−) cells. The p-eNOS(+)/CD31(+) cells and p-eNOS(+)/CD31(−) cells were localized in the neural fiber layer/ganglion cell layer (Fig. 7*K–N*).

Expression of ICAM-1, VCAM-1, CD11b, and CD18 Is Upregulated in the Retinas of Akita.PlGF$^{-/-}$ Mice

ICAM-1, VCAM-1, CD11b, and CD18 play important roles in regulating leukocyte-EC adhesion. We examined the protein and/or mRNA expression of these factors. The results showed that protein and/or mRNA expression of ICAM-1, VCAM-1, CD11b, and CD18 were increased in the retinas of both Akita and Akita.PlGF$^{-/-}$ mice (Fig. 8). The number of leukocytes adhering to the retinal vasculature was equal between Akita and Akita.PlGF$^{-/-}$ mice, both of which were significantly greater than WT or PlGF$^{-/-}$ nondiabetic mouse retina (Supplementary Fig. 7). These results suggest protection from diabetes complications due to PlGF deficiency is likely independent of suppression of leukocyte-EC adhesion or retinal leukostasis.

DISCUSSION

In the current study, we developed a novel Akita.PlGF$^{-/-}$ diabetic mouse strain. Investigation of the retinas from Akita.PlGF$^{-/-}$ mice suggests that PlGF deficiency prevents the diabetes complications of acellular capillary, retinal cell death, and BRB breakdown and also confers additional protection, as shown by the increased expression of ZO-1 and VE-cadherin. To gain further insight into the protective mechanisms, we investigated several important pathophysiological pathways and events in DR. First, we found that PlGF deletion in Akita mice led to an

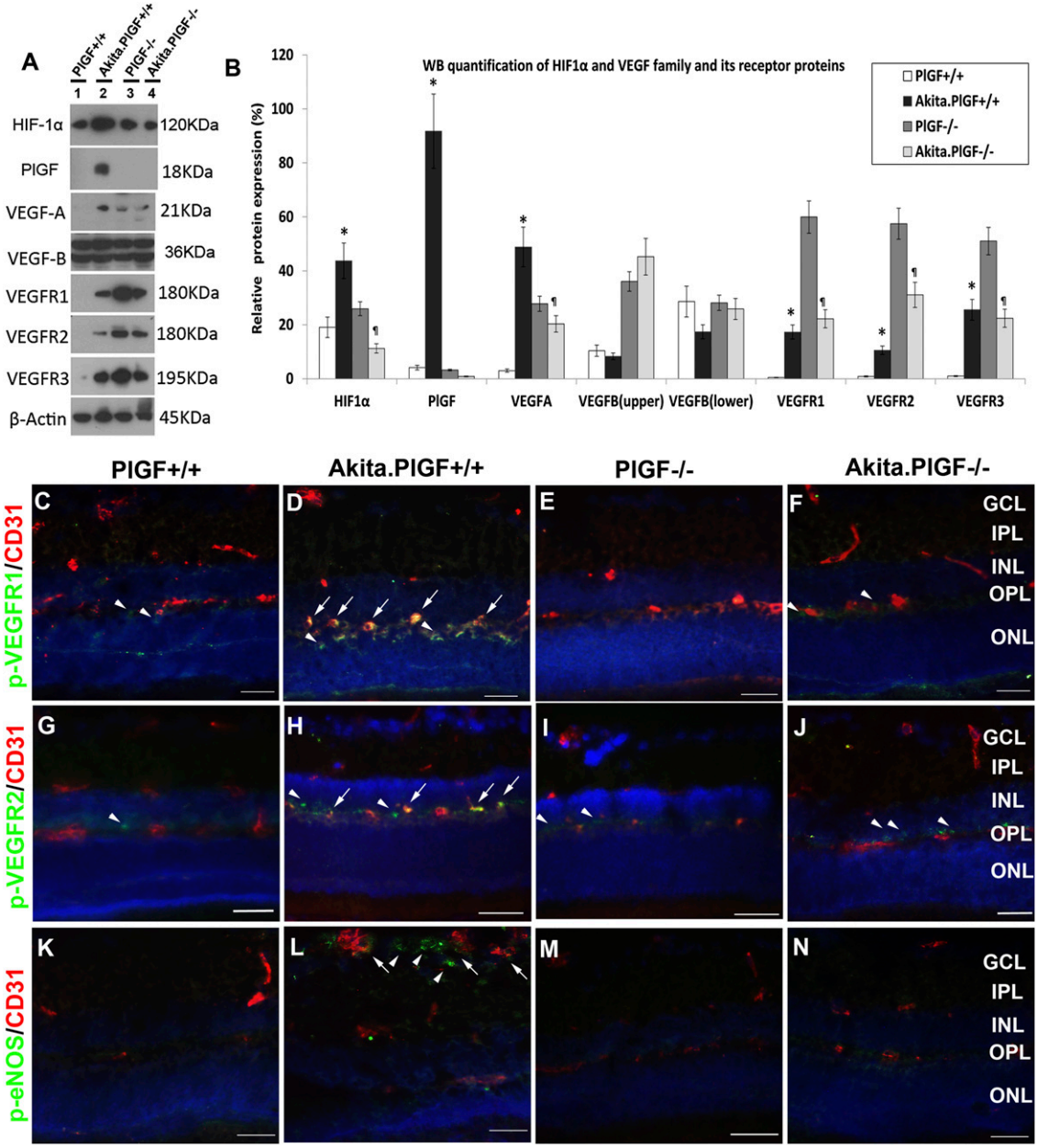

Figure 7—Inhibition of HIF1α-VEGF signaling pathway in the retinas of Akita.PlGF$^{-/-}$ mice. Six-month-old diabetic mice (~5-month diabetes duration) and nondiabetic littermate control mice were used for WB and IF. *A*: Example WB results for HIF1α, PlGF, VEGF-A, VEGF-B, VEGFR1, VEGFR2, and VEGFR3 are shown. The anti-β-actin antibody was used to probe the stripped protein membrane and was used as a controls for protein loading and quantification. Lane 1 is nondiabetic WT (PlGF$^{+/+}$); lane 2 is Akita.PlGF$^{+/+}$; lane 3 is nondiabetic PlGF$^{-/-}$; and lane 4 is Akita.PlGF$^{-/-}$. *B*: The WB quantification. The results were averaged from six independent mice and are expressed as mean relative expression ± SD (n = 6). *P < 0.05 (Akita vs. WT); ¶P < 0.05 (Akita.PlGF$^{-/-}$ vs. PlGF$^{-/-}$). Double-label IF staining was done for p-VEGFR1 and CD31 (*C–F*), p-VEGFR2 and CD31 (*G–J*), or p-eNOS and CD31 (*K–N*). Arrows indicate colocalization of phosphorylated protein and CD31 (yellow). Arrowheads indicate the immunoreactivity only for phosphorylated protein (green). Scale bar, 50 μm. GCL, ganglion cell layer; INL, inner nuclear layer; IPL, inner plexiform layer; ONL, outer nuclear layer.

increased Akt phosphorylation, which is an important survival factor and may contribute to the protective mechanisms. Second, we found that the expression of SHH and Ang-1 is corelated with that of VE-cadherin and ZO-1. The findings are in agreement with the previous reports that demonstrated SHH and Ang-1 play important roles in preserving the integrity of blood-brain barrier (34) and BRB (35), respectively. Third, we found that the HIF1 α-VEGF signaling pathway, which is the key mediator of diabetic retinal complications, was inhibited due to PlGF deficiency. Last, we found that leukocyte-EC adhesion, or retinal leukostasis, which is a relatively early

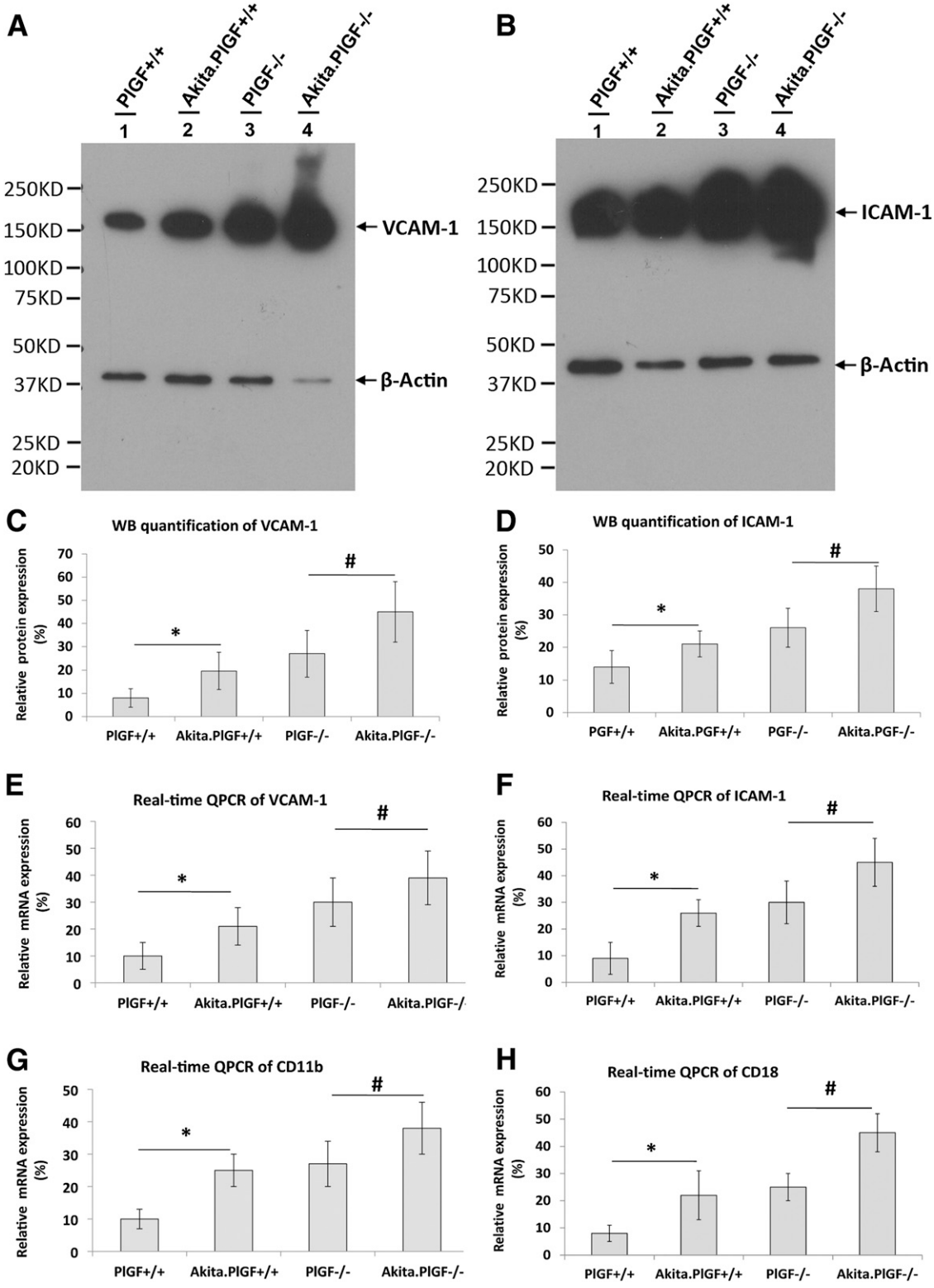

Figure 8—Increased expression of VCAM-1, ICAM-1, CD11b, and CD18 in the retinas of Akita mice and Akita.PlGF$^{-/-}$ mice. Protein lysates and total RNA were made from the retinas of 6-month-old mice (~5-month diabetes duration) and the nondiabetic littermate control mice. WB results for VCAM-1 (*A*) and ICAM-1 (*B*). The anti-β-actin antibody was mixed with anti-VCAM-1 or anti-ICAM-1 antibody and the mixture was used to probe the same protein membrane, serving as the internal control of protein loading and quantification of VCAM-1 (*A*) and ICAM-1 (*B*). WB quantification of VCAM-1 (*C*) and ICAM-1 (*D*) demonstrates a significant difference between diabetic and nondiabetic control mice. Relative mRNA expression of VCAM-1 (*E*), ICAM-1 (*F*), CD11b (*G*), and CD18 (*H*) represent the average from six independent samples and are expressed as mean ± SD (n = 6). *P < 0.05 (Akita.PlGF$^{+/+}$[Akita] diabetic mice vs. nondiabetic PlGF$^{+/+}$ [WT] mice); #P < 0.05 (Akita.PlGF$^{-/-}$ diabetic mice vs. nondiabetic PlGF$^{-/-}$ mice). QPCR, quantitative PCR.

event and contributes to the development of DR (36), was not suppressed by knocking out PlGF, and therefore, it is possible that the protection is independent of this inflammatory event. It is important to note that although retinal leukostasis has been shown to occur in the early stage in the streptozotocin-induced diabetic model (37), it also happens in the late stages in the Akita model.

The comparisons in this study were considered fairly robust since diabetic mice were always compared with nondiabetic control mice (Akita vs. WT and Akita.PlGF$^{-/-}$ vs. PlGF$^{-/-}$) to control for baseline differences owing to different genetic background, and nondiabetic control mice were always the male siblings of Akita diabetic mice. The four respective mouse strains were maintained by the breeding of Akita/C57 and Akita.PlGF$^{-/-}$/PlGF$^{-/-}$, and each breeding pair gave rise to offspring of which half were WT or PlGF$^{-/-}$ and half were diabetic Akita and Akita.PlGF$^{-/-}$; only the male diabetic mice were used for experimental analyses. To further ascertain the effects of PlGF deletion on diabetic retinal complications, we characterized the retinal vasculatures of the two nondiabetic mouse strains. The vascular cell density and pericyte number are comparative between PlGF$^{-/-}$ mice and WT mice (without statistically significant difference). Similarly, histopathological assessment demonstrated the gross anatomy of the retina looks similar among the mouse strains, without showing any retinal degeneration or other abnormities. Despite the similarities, it appears that there are differences in molecular composition and function. For example, the protein expression of VEGFR1–3 was increased in the nondiabetic PlGF$^{-/-}$ mice compared with the WT mice. The permeability of ^{3}H-mannitol (molecular weight 182 Da) was increased in PlGF$^{-/-}$ mice compared with the WT mice (approximately two- to threefold), using the lung and kidney as a reference (but not serum). However, the permeability of FITC-dextran (70 kDa) did not show any increase in the knockout mice. It is possible that the differences are attributed to the effect of long-term diabetes on the lung and kidney and the different molecular weight of the two tracers.

Currently, agents targeting VEGF are widely used for the treatment of vascular disorders, including DR. However, there is concern about potential side effects after a long-standing VEGF blockade because new evidence is emerging that VEGF is a survival factor for the choriocapillaris, retinal neurons, and RPE (38–40). One possibility is to target the upstream regulators of VEGF such as prolyl hydroxylase and HIF (41). Because prolyl hydroxylase and HIF regulate a broad spectrum of gene expression, inhibition of their activities could potentially protect the vasculature. Another possible therapeutic intervention would be inhibition of PlGF. In a study on PlGF$^{-/-}$ mice, Carmeliet and colleagues (6,42) showed that PlGF regulates angiogenesis and vascular permeability in pathological conditions. The results from the current study showed that deletion of PlGF led to not only the suppression of diabetes complications, but also an increase in junction and adhesion factors. These findings suggest that inhibition of PlGF signaling most likely produces the equivalent efficacy of blocking VEGF, but activation of protective factors in PlGF deficiency may also confer additional benefits.

Future work is needed to determine whether activation of Akt survival signaling and inhibition of VEGF signaling pathway are the causes of protection due to PlGF deficiency; how PlGF coordinates the interaction of VEGF, VEGFR1, and VEGFR2 in the background of DR; and the effect of PlGF deficiency upon other biological pathways involved in protection, such as tumor necrosis factor-α, the kallikrein-kinin system, and altered *O*-GlcNAc signaling. The Akita.PlGF$^{-/-}$ mouse is a good tool to use in the study of the in vivo effect of these kinds. From this study, it is now apparent PlGF plays a critical role in the pathogenesis of DR.

Acknowledgments. The authors thank Dr. Peter Carmeliet at VIB Vesalius Research Center, K.U. Leuven, Belgium, for providing PlGF$^{-/-}$ mice; Dr. Zhenhua Xu, Wilmer Eye Institute, for her helpful discussions about the WB experiments; and Dr. Junsong Gong, Wilmer Eye Institute, for his technical assistance.

Funding. This study was supported by research grants from the National Institutes of Health EY017164 (H.H.) and EY022383 (E.J.D.), Research to Prevent Blindness, and Wilmer Pooled Professor Funds (H.H.).

Duality of Interest. No potential conflicts of interest relevant to this article were reported.

Author Contributions. H.H. designed study, performed experiments, interpreted data, and wrote the manuscript. J.H., D.J., Y.W., Y.L., S.W., and E.J.D. performed experiments and interpreted data. G.A.L. and R.D.S. discussed the study and reviewed and edited the manuscript. H.H. is the guarantor of this work and, as such, had full access to all the data in the study and takes responsibility for the integrity of the data and the accuracy of the data analysis.

References

1. Antonetti DA, Klein R, Gardner TW. Diabetic retinopathy. N Engl J Med 2012; 366:1227–1239

2. Huang H, Gandhi JK, Zhong X, et al. TNFalpha is required for late BRB breakdown in diabetic retinopathy, and its inhibition prevents leukostasis and protects vessels and neurons from apoptosis. Invest Ophthalmol Vis Sci 2011;52: 1336–1344

3. Gao BB, Clermont A, Rook S, et al. Extracellular carbonic anhydrase mediates hemorrhagic retinal and cerebral vascular permeability through prekallikrein activation. Nat Med 2007;13:181–188

4. Semba RD, Huang H, Lutty GA, Van Eyk JE, Hart GW. The role of O-GlcNAc signaling in the pathogenesis of diabetic retinopathy. Proteomics Clin Appl 2014; 8:218–231

5. Maglione D, Guerriero V, Viglietto G, Delli-Bovi P, Persico MG. Isolation of a human placenta cDNA coding for a protein related to the vascular permeability factor. Proc Natl Acad Sci U S A 1991;88:9267–9271

6. Carmeliet P, Moons L, Luttun A, et al. Synergism between vascular endothelial growth factor and placental growth factor contributes to angiogenesis and plasma extravasation in pathological conditions. Nat Med 2001;7:575–583

7. Ohno-Matsui K, Yoshida T, Uetama T, Mochizuki M, Morita I. Vascular endothelial growth factor upregulates pigment epithelium-derived factor expression via VEGFR-1 in human retinal pigment epithelial cells. Biochem Biophys Res Commun 2003;303:962–967

8. Cao Y, Chen H, Zhou L, et al. Heterodimers of placenta growth factor/vascular endothelial growth factor. Endothelial activity, tumor cell expression, and high affinity binding to Flk-1/KDR. J Biol Chem 1996;271:3154–3162

9. Autiero M, Waltenberger J, Communi D, et al. Role of PlGF in the intra- and intermolecular cross talk between the VEGF receptors Flt1 and Flk1. Nat Med 2003;9:936–943
10. Dewerchin M, Carmeliet P. PlGF: a multitasking cytokine with disease-restricted activity. Cold Spring Harb Perspect Med 2012;2
11. Spirin KS, Saghizadeh M, Lewin SL, Zardi L, Kenney MC, Ljubimov AV. Basement membrane and growth factor gene expression in normal and diabetic human retinas. Curr Eye Res 1999;18:490–499
12. Khaliq A, Foreman D, Ahmed A, et al. Increased expression of placenta growth factor in proliferative diabetic retinopathy. Lab Invest 1998;78:109–116
13. Miyamoto N, de Kozak Y, Jeanny JC, et al. Placental growth factor-1 and epithelial haemato-retinal barrier breakdown: potential implication in the pathogenesis of diabetic retinopathy. Diabetologia 2007;50:461–470
14. Yonekura H, Sakurai S, Liu X, et al. Placenta growth factor and vascular endothelial growth factor B and C expression in microvascular endothelial cells and pericytes. Implication in autocrine and paracrine regulation of angiogenesis. J Biol Chem 1999;274:35172–35178
15. Mitamura Y, Tashimo A, Nakamura Y, et al. Vitreous levels of placenta growth factor and vascular endothelial growth factor in patients with proliferative diabetic retinopathy. Diabetes Care 2002;25:2352
16. Jonas JB, Jonas RA, Neumaier M, Findeisen P. Cytokine concentration in aqueous humor of eyes with diabetic macular edema. Retina 2012;32:2150–2157
17. Van de Veire S, Stalmans I, Heindryckx F, et al. Further pharmacological and genetic evidence for the efficacy of PlGF inhibition in cancer and eye disease. Cell 2010;141:178–190
18. Chang B, Hurd R, Wang J, Nishina P. Survey of common eye diseases in laboratory mouse strains. Invest Ophthalmol Vis Sci 2013;54:4974–4981
19. Mattapallil MJ, Wawrousek EF, Chan CC, et al. The Rd8 mutation of the Crb1 gene is present in vendor lines of C57BL/6N mice and embryonic stem cells, and confounds ocular induced mutant phenotypes. Invest Ophthalmol Vis Sci 2012;53:2921–2927
20. Huang H, Wahlin KJ, McNally M, Irving ND, Adler R. Developmental regulation of muscleblind-like (MBNL) gene expression in the chicken embryo retina. Dev Dyn 2008;237:286–296
21. Huang H, Shen J, Vinores SA. Blockade of VEGFR1 and 2 suppresses pathological angiogenesis and vascular leakage in the eye. PLoS ONE 2011;6:e21411
22. Huang H, Parlier R, Shen JK, Lutty GA, Vinores SA. VEGF receptor blockade markedly reduces retinal microglia/macrophage infiltration into laser-induced CNV. PLoS ONE 2013;8:e71808
23. Waters JC. Accuracy and precision in quantitative fluorescence microscopy. J Cell Biol 2009;185:1135–1148
24. Huang H, Frank MB, Dozmorov I, et al. Identification of mouse retinal genes differentially regulated by dim and bright cyclic light rearing. Exp Eye Res 2005;80:727–739
25. Laver NM, Robison WG Jr, Pfeffer BA. Novel procedures for isolating intact retinal vascular beds from diabetic humans and animal models. Invest Ophthalmol Vis Sci 1993;34:2097–2104
26. Wei Y, Gong J, Yoshida T, et al. Nrf2 has a protective role against neuronal and capillary degeneration in retinal ischemia-reperfusion injury. Free Radic Biol Med 2011;51:216–224
27. Dimaio TA, Wang S, Huang Q, Scheef EA, Sorenson CM, Sheibani N. Attenuation of retinal vascular development and neovascularization in PECAM-1-deficient mice. Dev Biol 2008;315:72–88
28. Gamble JR, Drew J, Trezise L, et al. Angiopoietin-1 is an antipermeability and anti-inflammatory agent in vitro and targets cell junctions. Circ Res 2000;87:603–607
29. Xia YP, He QW, Li YN, et al. Recombinant human sonic hedgehog protein regulates the expression of ZO-1 and occludin by activating angiopoietin-1 in stroke damage. PLoS ONE 2013;8:e68891
30. Costa G, Mazan A, Gandillet A, Pearson S, Lacaud G, Kouskoff V. SOX7 regulates the expression of VE-cadherin in the haemogenic endothelium at the onset of haematopoietic development. Development 2012;139:1587–1598
31. Reiter CE, Wu X, Sandirasegarane L, et al. Diabetes reduces basal retinal insulin receptor signaling: reversal with systemic and local insulin. Diabetes 2006;55:1148–1156
32. Hagberg CE, Falkevall A, Wang X, et al. Vascular endothelial growth factor B controls endothelial fatty acid uptake. Nature 2010;464:917–921
33. Hagberg CE, Mehlem A, Falkevall A, et al. Targeting VEGF-B as a novel treatment for insulin resistance and type 2 diabetes. Nature 2012;490:426–430
34. Alvarez JI, Dodelet-Devillers A, Kebir H, et al. The Hedgehog pathway promotes blood-brain barrier integrity and CNS immune quiescence. Science 2011;334:1727–1731
35. Nambu H, Nambu R, Oshima Y, et al. Angiopoietin 1 inhibits ocular neovascularization and breakdown of the blood-retinal barrier. Gene Ther 2004;11:865–873
36. Lutty GA. Effects of diabetes on the eye. Invest Ophthalmol Vis Sci 2013;54:ORSF81-7
37. Adamis AP, Berman AJ. Immunological mechanisms in the pathogenesis of diabetic retinopathy. Semin Immunopathol 2008;30:65–84
38. Saint-Geniez M, Maharaj AS, Walshe TE, et al. Endogenous VEGF is required for visual function: evidence for a survival role on müller cells and photoreceptors. PLoS ONE 2008;3:e3554
39. Kurihara T, Westenskow PD, Bravo S, Aguilar E, Friedlander M. Targeted deletion of Vegfa in adult mice induces vision loss. J Clin Invest 2012;122:4213–4217
40. Le YZ, Bai Y, Zhu M, Zheng L. Temporal requirement of RPE-derived VEGF in the development of choroidal vasculature. J Neurochem 2010;112:1584–1592
41. Huang H, Van de Veire S, Dalal M, et al. Reduced retinal neovascularization, vascular permeability, and apoptosis in ischemic retinopathy in the absence of prolyl hydroxylase-1 due to the prevention of hyperoxia-induced vascular obliteration. Invest Ophthalmol Vis Sci 2011;52:7565–7573
42. Luttun A, Brusselmans K, Fukao H, et al. Loss of placental growth factor protects mice against vascular permeability in pathological conditions. Biochem Biophys Res Commun 2002;295:428–434